Sapphire beamsplitters and test masses for advanced laser interferometer gravitational wave detectors

L. Ju [a], M. Notcutt [a], D. Blair [a], F. Bondu [b], C.N. Zhao [a]

[a] *Department of Physics, University of Western Australia, Nedlands, W.A. 6907, Australia*
[b] *Groupe VIRGO, Laboratoire de l'Accélérateur Linéaire, CNRS-IN2P3, Université de Paris-Sud, F-91405 Orsay Cedex, France*

Abstract

We present a feasibility study of using sapphire beamsplitters and test masses in laser interferometer gravitational wave detectors. The internal thermal noise, optical losses and birefringence effects are analysed. Suspension losses are investigated. Experimental data on birefringence is presented. The conclusions are generally positive.

1. Introduction

Laser interferometer gravitational wave detectors without resonant cavities in their arms but with very large power recycling gain and signal recycling gain [1–3] can be considerably simpler than the implementation of recycling in a Fabry–Perot Michelson interferometer as currently planned by the LIGO [4] and VIRGO [5] projects. High dual recycling gain can compensate for the absence of Fabry–Perot cavities in the arms as proposed by GEO project [6]. In this scheme the full resonant enhanced light power (carrier) must be transmitted through the beamsplitter. Therefore the beamsplitter becomes a critical component of the system, with full sensitivity to seismic and thermal noise. The optical scattering, optical absorption and thermal lensing [7] become the critical limitations on performance.

It is well known that the thermal and mechanical properties of sapphire make it an interesting material for use in test masses. The high thermal conductivity means that thermal lensing can be minimised, while the combination of its very high Young's modulus and low acoustic loss ensure that the internal resonant modes have high frequency and low thermal noise. Single crystal cylinders of 200–300 mm diameter and similar length are commercially available.

Until recently it was not known whether good optical super polishing could be achieved on sapphire. Now excellent results from polishing [8] and the absence of coating problems [9] seem to indicate that the material is useable from this perspective. Recent measurements [8] have also shown that the optical absorption coefficient can be as low as 3.5 ppm/cm in sapphire samples at 1 μm wavelength. This is superior to most samples of fused silica. However, several uncertainties remain before sapphire can be used with confidence in a laser interferometer.

In this paper we consider further aspects of interferometer design using a sapphire beamsplitter and end mirrors. We compare the thermal noise of a practical sapphire test mass with a similar silica test mass. We analyse methods of suspension of sapphire

test masses to prevent degradation of the internal mode Q-factors, while obtaining very low pendulum losses. We analyse the orientation requirements on sapphire optical components (imposed by the intrinsic birefringence of sapphire). Inhomogeneous and stress induced birefringence are also addressed.

Our conclusions are generally positive. We show that the internal thermal noise in a typical test mass is ~ 16 times lower than that of a similar silica mass. We show that a membrane suspension system can allow very high internal mode Q-factor to be achieved. Methods of bonding a membrane hinge to sapphire which should achieve this performance are discussed. However, there is a trade off between internal mode Q, longitudinal suspension mode frequency and rocking frequency. To achieve a worst case internal mode Q equal to the highest observed Q-factor in sapphire at room temperature ($Q > 10^8$ [10]), a membrane with a Q-factor of 10^5 is required.

Our analysis also shows that the orientation requirements on the sapphire crystal are within reasonable operational tolerances while our measurements show that as long as stress birefringence is avoided, adequate birefringence homogeneity can be achieved. Assuming an interferometer operating at 1 μm wavelength, Rayleigh scattering losses of almost 20 ppm/cm are difficult to avoid. A total absorption loss of ~ 60 ppm can be anticipated in a sapphire beamsplitter, depending on the material thickness. The high Rayleigh scattering sets limits on the maximum recycling gain.

2. Thermal noise of a sapphire test mass

2.1. Internal modes

According to the fluctuation–dissipation theorem [11], the thermal noise due to the internal resonant of the test mass can be expressed by [12]

$$\Delta x^2 = \frac{4k_BT}{\omega} \sum_i \frac{\Phi_i(\omega_i)\omega_i^2}{M_i\left[\left(\omega_i^2 - \omega^2\right)^2 + \Phi_i^2(\omega)\omega^4\right]},$$

(1)

where ω_i and M_i are the angular frequency and the equivalent mass of the ith mode respectively. Here

Table 1
The first nine internal modes and the equivalent masses of a cylindrical sapphire test mass; $d = 200$ mm, $H = 200$ mm (~ 25 kg), beam size 2 cm

frequency (Hz)	M_i (kg)	$M_i\omega_i^2$
22652	9.13	1.85×10^{11}
29284	17.8	6.04×10^{11}
36997	91.9	4.96×10^{12}
46468	2.45	2.09×10^{11}
54115	2.75	3.18×10^{11}
27480	20.7	6.17×10^{11}
34385	4.24	1.98×10^{11}
45411	8.33	6.78×10^{11}
52506	16.9	1.84×10^{12}

the structural damping mechanism is assumed, with loss factor $\Phi(\omega_i) = 1/Q_i$, constant over a large frequency range [13,14]. For frequencies $\omega \ll \omega_i$, the thermal noise can be expressed as

$$\Delta x^2 = \frac{4k_BT}{\omega} \Phi(\omega) \sum_i \frac{1}{M_i\omega_i^2} = \frac{4k_BT}{\omega} \frac{\Phi(\omega)}{M_{eq}\omega_{eq}^2}.$$

(2)

The internal resonant modes of a sapphire test mass can be calculated by numerical methods [15–17] based on the theory of elasticity in continuous media [18]. We have assumed a free mass model and used the program "CYPRES" [15] to calculate various test mass configurations. "CYPRES" allows the effective mass and frequency of the test mass normal modes to be calculated. For a cylindrical sapphire test mass with diameter of $d = 200$ mm, thickness of $H = 200$ mm (~ 25 kg) and a beam size of 2 cm, the first nine internal resonances below 60 kHz and the equivalent masses are listed in Table 1. The high internal resonant frequencies in the sapphire test mass are very important in reducing their thermal noise contribution.

We tested for convergence of the thermal noise calculation by integrating over the first 200 normal modes, and compared the results with that of a silica test mass of the same dimensions. The values of $M_{eq}\omega_{eq}^2$ for sapphire and silica test masses of the same dimensions are 16.3×10^9 and 2.9×10^9 respectively. It can be seen that the value $M_{eq}\omega_{eq}^2$ of a sapphire test mass is 6.54 times greater than that of a silica test mass.

The highest internal mode Q-factor reported in silica is 7×10^6 [19]. This compares with 3×10^8
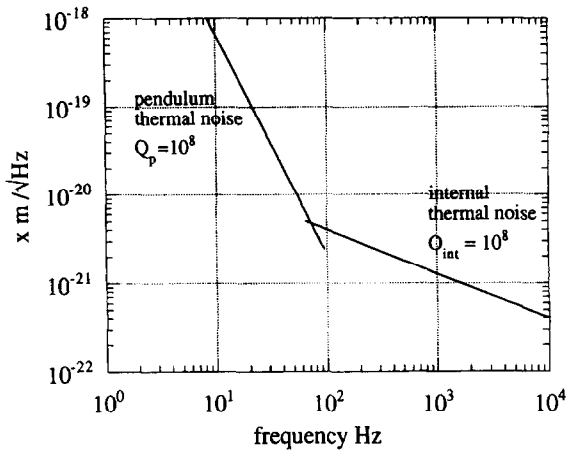
Fig. 1. Predicted thermal noise of a sapphire test mass. The intrinsic Q-factor of the test mass is chosen as 10^8. The pendulum Q factor is chosen as 10^8 with a niobium membrane flexure Q-factor of 10^5.

reported for sapphire by Braginsky et al. [10]. The reduced losses, combined with the increased values of $M_{eq}\omega_{eq}^2$ of sapphire means that the thermal noise amplitude of this sapphire test mass will be a factor of more than 16 times better than that of a silica test mass with the same dimensions,

$$\sqrt{\frac{Q_{sapp}\left(M_{eq}\omega_{eq}^2\right)_{sapp}}{Q_{silica}\left(M_{eq}\omega_{eq}^2\right)_{silica}}} > 16.$$

In this analysis we have assumed that the incident laser light is concentric with the test mass. In reality it is advantageous to illuminate the test mass at the centre of percussion to reduce pendulum thermal noise contributions as discussed below. The offset of the beam and the relative beam size will alter the integrated thermal noise by a small factor. To achieve the optimum sensitivity of a laser interferometer it is essential that the test mass combines the high internal mode Q-factor discussed above, with extremely high pendulum Q-factors. Fig. 1 shows a typical target noise level. In the next section we discuss means of achieving this.

2.2. Flexure suspension of test masses

Braginsky measured the high Q-factor [10] in sapphire by suspending it from fine wires of tungsten or silk. However, our extensive experience with

resonant mass gravitational wave detectors has led us to be pessimistic about this approach, mainly due to the poor definition of the boundary conditions between the suspension fibre and the test mass, which can lead to acoustic upconversion and excess losses. For this reason we have proposed alternative suspension techniques which are capable of achieving the required low losses without the use of wires. In the following discussion, we present an analysis of such an alternative suspension system.

Fig. 2 shows a diagram of this suspension concept. With a cylindrical test mass of diameter of $d = 200$ mm, thickness of $H = 200$ mm, this compound pendulum will have a resonant frequency of 1.3 Hz. The centre of percussion of this pendulum, at which the transfer function will be the same as a simple pendulum, will be at 43 mm below the centre of mass.

The advantage of using a short thin membrane flexure is that it has very high violin string modes, low flexural spring constant and very low thermoelastic loss. It has been shown previously that a membrane flexure allows enhanced pendulum Q-factors [20,21] compared with wire suspension. The pendulum Q-factor with a thin membrane flexure is given by

$$Q_p = Q_0\left(\frac{3MgL^2}{Eat^3}\right)^{1/2},\qquad(3)$$

where M is the mass of the pendulum, L, a, t and E are the length, width, thickness and Young's modulus of the membrane, respectively.
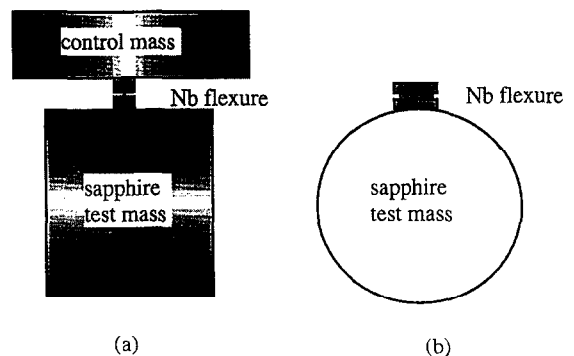

(a)   (b)

Fig. 2. A practical design for a sapphire beamsplitter. (a) Side view; (b) front view. The suspension element is a thin niobium membrane flexure, typically 25 μm thick, 2 mm long and 4 cm wide.

The data in Fig. 1 for the pendulum mode thermal noise correspond to a niobium flexure for which the intrinsic Q-factor of the material is 10^5 (~ 40 times less than the bulk niobium Q-factor at room temperature). The "violin string" modes of the short membrane are very high (~ 100 kHz), leaving a "clean window" for gravitational wave detection. At 10 Hz the noise is mainly pendulum mode thermal noise which reaches a level of 7×10^{-19} m/$\sqrt{Hz}$, while at 200 Hz the internal resonant modes thermal noise dominate at a level of $\sim 4 \times 10^{-21}$ m/$\sqrt{Hz}$. We believe that a flexure suspension can be constructed as described below.

2.3. Bonding of the flexure to the test mass

In principle, due to the very high achievable pendulum Q-factor [21], a niobium membrane suspended sapphire test mass can give optimum noise performance at low frequencies. However, to realise such a system, it is necessary to find a practical solution to the fabrication and assembly of such a suspension system, and to confirm whether the internal mode Q-factor of the test mass can be maintained, and whether the total thermal noise is sufficiently low. The internal modes can lose energy through the membrane. Large lossy components will

degrade the internal mode Q-factor, and in addition the imperfect clamping of mechanical components will cause excess acoustic losses. In particular the imperfect bonding of the flexure to the test mass will cause additional loss in the pendulum.

We propose the use of well established ceramic to metal sealing techniques to overcome this problem. Numerous methods have been developed for different applications [22]. Among these techniques, active metal seals, diffusion seals and solder seals are of interest for our application. The refractory properties of niobium and sapphire, their satisfactory thermal expansion match from liquid helium temperature [23] to 2000°C [24], and the low acoustic losses of both materials makes niobium appear ideally suited for bonding to sapphire for the purpose of creating a low loss flexure pivot suspension.

Sapphire to niobium seals using active metal brazing with titanium and vanadium allows high strength bonding at ~ 1800°C [24]. Active metal brazing alloys such as Incusil-ABA® (Indium-copper-silver) and Cusil-ABA™ (Copper-silver) can create a high integrity bond at 700–830°C [25]. Preliminary test using Incusil brazing has resulted a joint between sapphire and niobium with strength > 150 MPa.

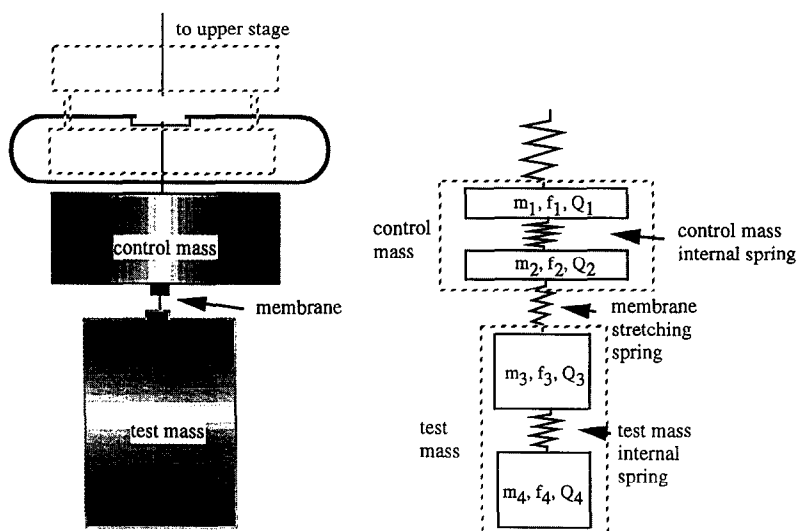We have preliminarily investigated direct diffusion bonding between sapphire and niobium at

Fig. 3. Model one: test mass suspended directly under control mass. A four stage spring mass model is used. Spring 1: spring of the whole isolator; spring 2: internal spring of the control mass; spring 3: test mass membrane flexure stretching spring; spring 4: equivalent test mass internal spring.
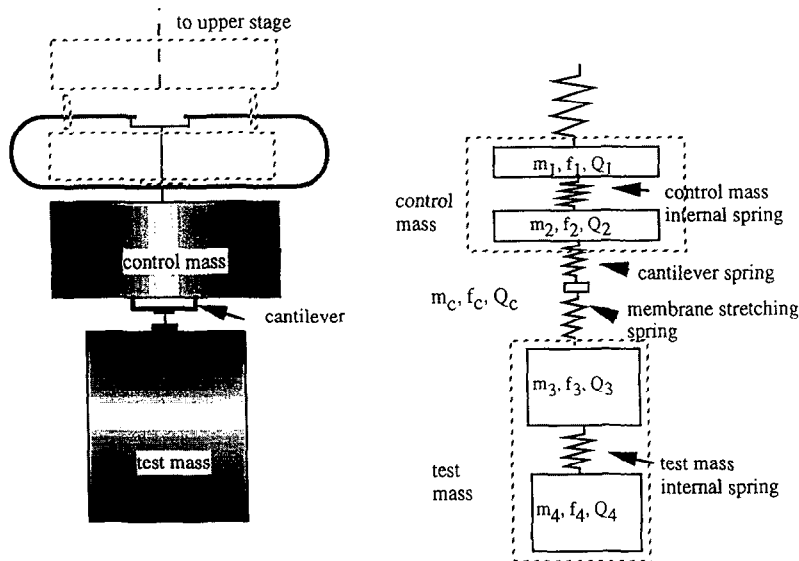
Fig. 4. Model 2: test mass suspended under a low loss, low mass cantilever which in turn is connected to the control mass. A five stage spring and mass model is used. Spring C: cantilever spring; the other elements are the same as in model 1 (Fig. 3).

1400°C. Preliminary experiments have achieved yield strength ~ 15 MPa for joints created at a contact pressure of about 5 MPa. Higher strength joints can be expected using higher temperatures and surface pressure. It remains to determine whether any of the above joints have sufficiently low acoustic losses.

Using one of the above methods, it is possible that very low mass niobium flexure components can be attached to the edge of a sapphire test mass, to create a high integrity mechanical suspension structure. We go on to show that such a structure will allow a high internal mode Q-factor to be maintained, and that the total test mass thermal noise can be exceptionally low.

3. The effect of low Q-factor upper stages on sapphire test mass internal Q-factor

In practice a test mass will be suspended from a vibration isolation stack as shown in Fig. 1. Usually the intrinsic Q-factor of the isolator elements will be low. We assume here the use of metal cantilever spring vibration isolators [26] with normal mode Q-factors ~ 10^3. Suppose the last isolation stage (control mass) has a mass of 40 kg and internal resonant frequency of the order 10^3 Hz. From Sec-

tion 1.1, the lowest internal resonant frequency of a 25 kg sapphire test mass can exceed 20 kHz. It is possible, however, that the internal mode Q-factor of the test mass will be degraded through coupling to the internal mode of the control mass. Such Q-factor degradation is likely to degrade the test mass thermal noise. To assess this problem, the system was modelled in one dimension, using lumped mass and spring elements [27]. Two models were considered. One consists of a directly coupled system, using a moderately low loss membrane hinge. The second consists of one in which a small cantilever stage is inserted between the control mass and test mass to provide some degree of vertical isolation. Figs. 3 and 4 show the two mechanical systems and their models (see the figure captions for full details).

To examine the effect of Q degradation of the test mass, we assume that the test mass has an extremely high intrinsic Q-factor ($Q = 10^{10}$). Other parameters of the model are $f_1 = 2$ Hz, $f_2 = 10^3$ Hz, $f_3 = 300$ Hz [1], $f_4 = 10^4$ Hz ($f_c = 100$ Hz); $m_1 = m_2 = 25$ kg,

---

[1] The stretching mode frequency of the foil flexure f_3 is chosen for a membrane flexure length of 2 mm, width of 4 cm and thickness of 25 μm. The membrane is thus stretched to 25% of its yield strength.
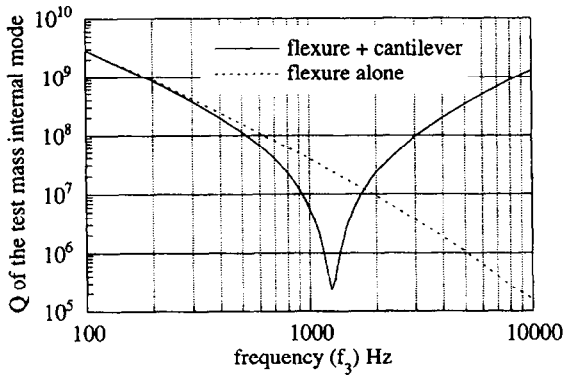
Fig. 5. Test mass internal resonant Q-factor as a function of the mass of the cantilever stage. The dotted line is that of a system without cantilever stage. It can be seen that the Q-factor of "flexure + cantilever" model exceeds that of "flexure alone" model only when the cantilever stage mass is impractically small.

Fig. 6. Test mass internal resonant Q-factor as a function of the membrane flexure (with $f_3 = 300$ Hz).

$m_3 = m_4 = 12.5$ kg ($m_c = 0.1$ kg); $Q_1 = 10^3$, $Q_2 = 10^3$, $Q_3 = 10^5$, $Q_4 = 10^{10}$ ($Q_c = 10^5$).

Using the above parameters, the test mass internal mode Q for four stages (without the small cantilever) is 4.25×10^8. With the small cantilever added, the test mass internal mode Q is (almost) independent of Q_2 and f_2 (the Q-factor and internal frequency of the control mass). It is also independent of Q_c and f_c (the cantilever stage Q-factor and frequency). The test mass internal mode Q is dependent on the mass of the cantilever stage (m_c), the frequency of the membrane stage(f_3), and, of course, on the Q-factor of membrane flexure Q_3. The results are shown in Figs. 5 and 6.

In the model with a small cantilever intermediate stage, the anticipated Q enhancement of the intermediate stage can only be achieved for unrealistically low mass cantilevers. The test mass internal Q-factor is degraded strongly when the cantilever mass and membrane stretching frequency create a resonant coupling of energy from the test mass to the control mass. This implies that to achieve a high coupled mode Q-factor, there is no advantage in adding a low mass stage in between the test mass and the control mass.

Since it is the overall thermal noise of the system which is of importance to the sensitivity of the laser interferometer detectors, we modelled the vertical and horizontal thermal noise for the above two cou-
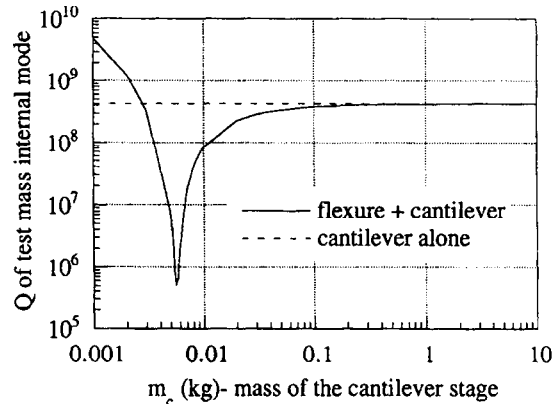
pled systems (Figs. 3 and 4). The horizontal models have the following parameters: $f_1 = 1$ Hz, $f_2 = 10^3$ Hz, $f_3 = 1$ Hz (see footnote 1), $f_4 = 10^4$ Hz ($f_c = 100$ Hz); $m_1 = m_2 = 25$ kg, $m_3 = m_4 = 12.5$ kg ($m_c = 0.1$ kg); $Q_1 = 10^3$, $Q_2 = 10^3$, $Q_3 = 10^8$ (pendulum Q-factor), $Q_4 = 10^8$ (internal Q-factor) ($Q_c = 10^5$).

The vertical to horizontal coupling is obtained by determining the differential thermal noise across the test mass internal spring (see Figs. 3 and 4), corrected by the Poisson ratio of the test mass (0.29). The results are shown in Figs. 7 and 8.
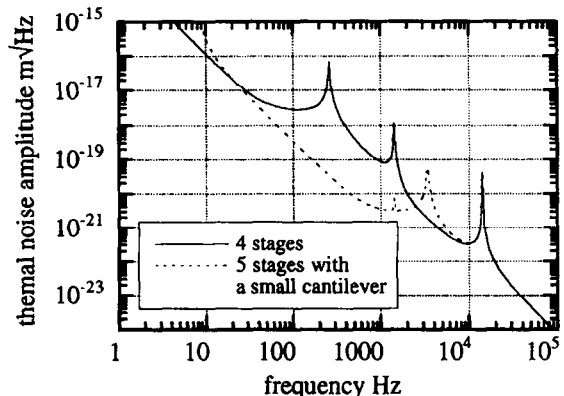

Fig. 7. Vertical thermal noise of the system shown in Figs. 3 and 4. The amplitudes of the resonances are not accurate because of the plot points problem.
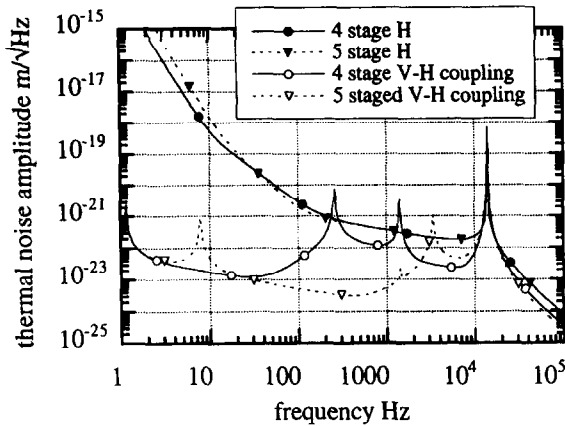
Fig. 8. Horizontal thermal noises of the systems shown in Figs. 3 and 4. The vertical to horizontal coupling is obtained by determining the differential thermal noise across the test mass internal spring (see Figs. 3 and 4), corrected by the Poisson ratio of the test mass (0.29).

It is interesting to note that the vertical thermal noise of "flexure only" model is degraded by the presence of the membrane stretching mode in the middle of the spectrum. However, this will not degrade horizontal thermal noise through vertical to horizontal coupling. The horizontal thermal noise of the model with a small cantilever added is slightly degraded by the presence of the cantilever at low frequency. We conclude that the simple membrane suspension is the better choice because of the simplicity and satisfactory thermal noise performance. From the viewpoint of internal thermal noise, it is
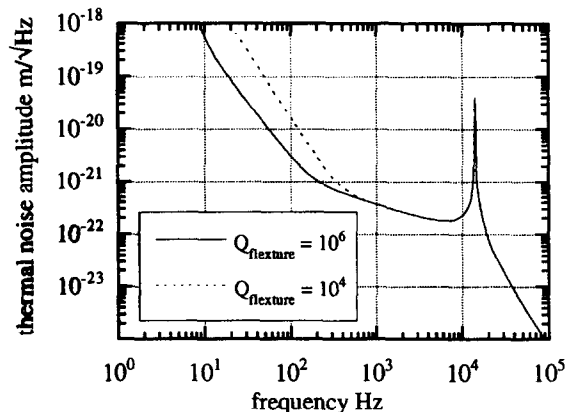

Fig. 9. Comparison of the thermal noise of membrane suspended sapphire test mass with different membrane flexure Q-factors.

possible to use a lower Q-factor membrane, but this is at the expense of low frequency pendulum noise as shown in Fig. 9.

The high internal mode Q-factor in the "flexure only" model indicates that an internal resonant mode Q-factor of 10^8 of the sapphire test mass could be observed in the isolation and suspension system, assuming that the intrinsic Q-factor of the sapphire material is as reported in the literature [10].

4. Optical losses in sapphire

Having considered the mechanical properties of the suspension of sapphire test masses, we now discuss the optical characteristics of sapphire mirrors and beamsplitter.

4.1. Absorption

In a recycling interferometer, the full resonant power must pass through the beamsplitter. It is crucial that the optical absorption of the beamsplitter is small to keep power losses small and minimise thermal lensing by the beamsplitter. Recent tests on sapphire have shown an absorption coefficient of $\alpha \sim 3.5$ ppm/cm at 1 μm [9]. This is superior to most published absorption coefficients of fused silica samples [28]. However, a recent result in ultra pure silica gives an absorption $\alpha \sim 1$ ppm/cm [29]. With a thickness of 20 cm, the absorption of a sapphire beamsplitter will be ~ 60 ppm. With such a small thermal absorption and high thermal conductivity of sapphire, the thermal lensing of the sapphire beamsplitter will be small.

4.2. Rayleigh scattering

Apart from the thermal absorption, there is an additional optical loss by scattering due to density fluctuations. The reduction in intensity is given by

$$I = I_0 \exp[-(\alpha + \gamma)x], \qquad (4)$$

where γ is the scattering coefficient.

A detailed calculation using a computer program "OPTIMATR" [30] gives a Rayleigh scattering limit for sapphire (o-ray at room temperature) of $\gamma = 18$

ppm/cm at 1 μm. This is much higher than the Rayleigh scattering limit in silica of 1.88 ppm/cm [28]. It can be seen that the Rayleigh scattering loss is much greater than the absorption loss and thus sets the limit to the achievable power recycling. However, the Rayleigh scattering does not contribute to thermal lensing.

4.3. Effects of sapphire birefringence for beamsplitters

The intrinsic birefringence property of sapphire is one disadvantage. For a perfect alignment the polarisation axis of the light will be aligned with one of the sapphire crystal's axes of symmetry. A relative misalignment of the polarisation and crystal axes will cause the light to become elliptically polarised as it travels through the sapphire. Misalignment may be caused by fluctuations of the beam or motion of the beamsplitter. From our experience of isolation systems for interferometers, this motion is likely to be the residual normal mode motion of rocking and rotation after electronic damping. In our system these motions have angular magnitudes of a few microradians.

Sapphire is a uni-axial crystal with a c-axis of rotational symmetry. A number of combinations of polarisation, beam direction and c-axis alignment are possible. We have chosen the polarisation (e) to be parallel to the c-axis (c) and the propagation to be in the a-axis plane. Suppose the polarisation of the light (e) has a small angle ψ with the c-axis as shown in Fig. 10, the ellipticity introduced to the beam that double-passes the beamsplitter will lead to
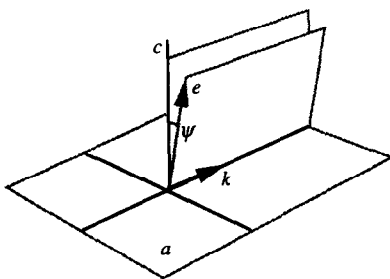

Fig. 10. Illustration of light polarisation direction in relation to sapphire axis. Here c direction is the c-axis of the crystal, e is the light polarisation direction and k is the light propagation direction.

imperfect interference. The non-interfered light escapes from the interferometer out of each output port. In a power-recycled interferometer the power loss is detrimental to the performance of the system as it limits the power enhancement by resonant reflection of the bright output. For this reason we investigate the losses caused by birefringence in a sapphire beamsplitter.

The fraction of lost power is

$$P_{lost}/P = \sin^2\phi \, \sin^2 2\psi, \tag{5}$$

where ψ is the angle between c and e, and 2ϕ is the difference in the phase shift of the light along the orthogonal crystal axes. For sapphire and laser light of $\lambda = 1064$ nm, the phase shift will be

$$\phi = 2\pi/270 \, \mu m. \tag{6}$$

Since this is such a quickly varying function it will be set to its maximum value, 1. Then

$$P_{lost}/P = \sin^2 2\psi \approx 4\psi^2. \tag{7}$$

For angles less than 100 μrad, which is easy to realise in our suspension systems, this loss will be significantly less than other loss sources such as mirror losses and curvature mismatch. We conclude that the birefringence of sapphire is not a detrimental factor in using it as a beamsplitter substrate.

On the other hand, the inhomogeneity of sapphire and stress in it can cause birefringence. We have preliminarily investigated the birefringence of a small $10 \times 10 \times 25$ mm^3 sapphire sample, using a similar method to that of Logan et al. [31], which consisted of a half-wave plate, polarisers and a phase compensator. The observed phase shift between the ordinary ray and extraordinary ray due to birefringence is shown in Fig. 11a. The star shaped pattern observed is a characteristic of stress birefringence due to surface strain. Because of the small sample size this penetrated to the centre of the sample. The phase shift in the centre is within $0.5°$ ($0.2°$/cm) as shown in Fig. 11b.

In large sapphire samples, such as 20 cm diameter and 10 cm thick, the stress at the centre is expected to be much smaller. From our data we have attempted to estimate the birefringence inhomogeneity contribution which will add noise to the stress birefringence pattern observed. We estimate an upper limit for this contribution. $\sim (0.02°–0.04°)$/cm, which is of the order of our measurement uncer-

▨	4-5
▩	3-4
▩	2-3
▩	1-2
☐	0-1
▨	-1-0
☐	-2–1
■	-3–2
▨	-4–3
☐	-5–4

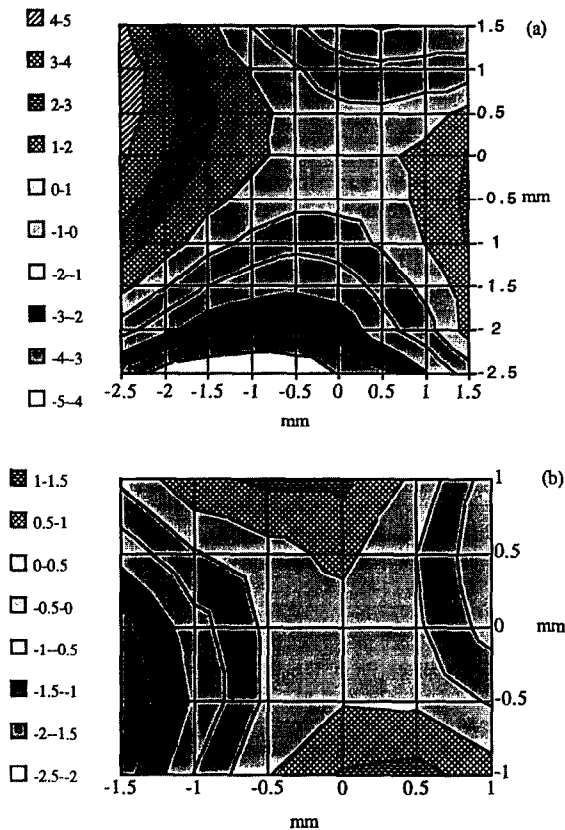|	
▩	1-1.5
▩	0.5-1
☐	0-0.5
☐	-0.5-0
☐	-1–0.5
■	-1.5–1
▨	-2–1.5
☐	-2.5–2

Fig. 11. Phase shift map of the ordinary ray and extraordinary ray in the sapphire sample due to birefringence. (a) Map of the whole piece; (b) enlarged central area. The grey scale indicates the total observed phase shift in degrees.

tainty. This limit can be compared with experimental requirements in interferometer detectors. If the average mirror loss is $\sim 10^{-5}$ per mirror [31], the total mirror loss would be $\sim 10^{-3}$ for 100 bounces of light in one arm. For the loss due to inhomogeneous birefringence to be of the same order or less than other mirror losses, the total inhomogeneous birefringence phase shift should be smaller than 2° in a beamsplitter. The above results in a small sapphire sample seem promising since they result in a stress induced birefringence phase shift of $\sim 2°$ and an estimated inhomogeneous birefringence of < 1° in a 10 cm thick test mass. In large sapphire samples, such as 20 cm diameter and 10 cm thick, the stress at the centre is expected to be much smaller. However, as pointed out in Ref. [31], the technology for developing low loss mirror is improving, the inhomoge-

neous and stress induced birefringence will become increasingly important. It is important that further more accurate measurements on large sapphire samples be made to obtain definitive results.

5. Conclusion

Sapphire with its excellent mechanical and thermal properties is an attractive material to use for beamsplitter and test masses in laser interferometer gravitational wave detectors. We have shown that the birefringence of sapphire should not be a problem with our well controlled vibration isolation and suspension systems. However, the birefringence induced by stress and inhomogeneity in a large piece of sapphire needs further investigation to confirm that the inhomogeneous phase shift is sufficiently small.

The internal thermal noise amplitude of a sapphire test mass will be ~ 16 times better than that of a fused silica test mass with the same dimensions. The end-supported beamsplitter will have its fundamental longitudinal mode most severely degraded by the suspension system. The model used here therefore represents the worst case Q-degradation of the beamsplitter. A longitudinal frequency of 300 Hz corresponds to a membrane of only one or two millimetres length. The results show that the test mass can maintain a Q-factor $\sim 10^8$ when suspended in this way. A referee has pointed out that reported ultrahigh Q-factors in sapphire are unreliable. For this reason we are already undertaking a testing program to confirm the intrinsic Q-factor of sapphire. The availability of much purer sapphire material than originally reported by Braginsky et al. [10], with microwave Q-factor 1–2 orders of magnitude better [32] than they reported, leads us to be optimistic that even lower acoustic losses may be achievable in pure material.

Further work is required to confirm the practicality of the proposed suspension systems discussed here, and to determine whether large sapphire samples maintain the optical performance observed in small scale samples. If this work is confirmed and realised, the total local noise sources in laser interferometers can be reduced by a factor ~ 16. This means that there is a substantial margin for creating

optical readout systems capable of achieving this sensitivity advantage, for example, by using narrow band resonant recycling schemes. In particular the laser interferometer gravitational wave detectors can be reduced in size by more than an order of magnitude while maintaining the sensitivity predicted using silica test masses. Conversely, the 3–4 km interferometers currently under construction can be enhanced in sensitivity by a similar margin. In both cases the uncertainty principle sets a fundamental limit which is uncomfortably close to the practical limits discussed here.

Acknowledgement

References

[1] R.P. Drever, Interferometric detectors of gravitational radiation, in: Gravitational radiation, eds. N. Deruelle and T. Piran, (North-Holland, Amsterdam, 1983).
[2] B.J. Meers, Phys. Rev. D 38 (1988) 2317.
[3] B.J. Meers and K.A. Strain, Phys. Rev. Lett. 66 (1991) 1391.
[4] A. Abramovici, W.E. Althouse, R.W.P. Drever, Y. Gürsel, S. Kawamura, F.J. Raab, D. Shoemaker, L. Sievers, R.E. Spero, K.S. Thorne, R.E. Vogt, R. Weiss, S.E. Whitcomb and M.E. Zuker, Science 256 (1992) 325.
[5] B. Mours, The VIRGO project contribution to Europhysics Conference on High energy physics, 1993.
[6] K. Danzmann et al., GEO 600: A 600 m laser interferometric gravitational wave antenna, in: Proc. 1st Eduardo Amaldi Conf. on Gravitational wave experiments, eds. E. Coccia, G. Pizzella and F. Ronga (World Scientific, Singapore, 1995).
[7] W. Winkler, K. Danzmann, A. Rüdiger and R. Schilling, Phys. Rev. A 44 (1991) 7022.
[8] D.G. Blair, M. Notcutt, C.T. Taylor, E.K. Wong, C. Walsh, A. Leistner, J. Seckold and J.-M. Mackowski, Development of low loss sapphire mirrors, submitted to Appl. Opt. (1995).
[9] D.G. Blair, F. Cleva and N. Man, Optical absorption measurements in monocrystalline sapphire at 1 micron, submitted to Opt. Mater. (1995).
[10] V.B. Braginsky, V.P. Mitrofanov and O.I. Panov, Systems with small dissipation (Univ. Chicago Press, Chicago, 1985).
[11] H.B. Callen and T.A. Welton, Phys. Rev. 83 (1951) 34.
[12] P.R. Saulson, Phys. Rev. D 42 (1990) 2437.
[13] P.R. Saulson, R.T. Stebbins, G.D. Dumont and S.E. Mock, Rev. Sci. Instrum. 65 (1994) 182.
[14] A. Gillespie and F. Raab, Phys. Lett. A 178 (1993) 357.
[15] A.E.M. Love, A treatise on the mathematical theory of elasticity (Dover, New York, 1944).
[16] F. Bondu and J.Y. Vinet, Phys. Lett. A 198 (1995) 74.
[17] A. Gillespie and G. Raab, Phys. Rev. 52 (1995) 577.
[18] This calculation of sapphire makes the approximation that the material is isotropy. Crystalline anisotropy will contribute a small error to the magnitude of $M_{eq}\,\omega_{eq}$.
[19] V.B. Braginsky, V.P. Mitrofanov and O.A. Okhrimenko, JETP Lett. 55 (1992) 432.
[20] W. Martin, Experiments and techniques for the detection of gravitational and pulsed electromagnetic radiation from astrophysical sources, Ph.D. Thesis, University of Glasgow (1987).
[21] D.G. Blair, L. Ju and M. Notcutt, Rev. Sci. Instrum. 64 (1993) 1899.
[22] W.H. Kchi, Handbook of materials and techniques for vacuum devices (Reinhold, New York, 1967).
[23] P.J. Veitch, Development and preliminary operation of a cryogenic gravitational radiation detector, Ph.D. Thesis, University of Western Australia.
[24] L. Bogart and I. Ben-Zvi, Rev. Sci. Instrum. 45 (1974) 713.
[25] WESGO Technical Ceramics and Brazing Alloys, Technical Data (1995).
[26] L. Ju and D.G. Blair, Rev. Sci. Instrum. 65 (1994) 3482.
[27] M.E. Tobar, Phys. D 28 (1995) 1728.
[28] B.Y. Baurès and C.N. Man, Opt. Mater. 2 (1993) 241.
[29] VIRGO project, private communications (1996).
[30] Crystal Systems, private communications (1995), which referenced W.J. Tropf and M.E. Thomas at The Johns Hopkins University.
[31] J.E. Logan, N.A. Robertson and J. Hough, Opt. Commun. 107 (1994) 342.
[32] A.N. Luiten, A.G. Mann and D.G. Blair, Electro. Lett. 29 (1993) 879.